ARTICLE

Synthesis, Crystal Structure and DNA-Binding Property of a New Cu(II) Complex Based on 4-(Trifluoro-methyl)nicotinic Acid①

SHAN Feng-Lin[a, b] SONG Huan[a, b] GAO Xue-Zhi[a, b]
LI Bing[a, b] MA Xiao-Xia[a, b②]

[a] (*State Key Laboratory of High-efficiency Utilization of Coal and Green Chemical Engineering, Ningxia University, Yinchuan* 750021, *China*)

[b] (*Department of Chemistry & Chemical Engineering, Ningxia University, Yinchuan* 750021, *China*)

ABSTRACT A new complex $[Cu_{1.5}(tfc)_3(H_2O)_4]\cdot 3H_2O$ (**1**, Htfc = 4-(trifluoro-methyl) nicotinic acid) has been synthesized and characterized by X-ray single-crystal diffraction, elemental analysis, IR spectra and thermogravimetric analysis. **1** belongs to orthorhombic system, space group *Pccn* with a = 44.507(2), b = 10.7710(6), c = 11.7544(7) Å, V = 5634.9(6) Å^3, Z = 1, D_c = 1.803 mg·cm^{-3}, F(000) = 3068, μ = 1.266 mm^{-1}, the final R = 0.0488 and wR = 0.1103 with $I > 2\sigma(I)$. The Cu(II) ion is coordinated by two N and two O atoms from different Htfc as well as two O atoms from two coordinated water molecules, forming a 0D motif with distorted octahedral geometry. The adjacent 0D units are linked into 2D structures through bridge connection coordination mode. In addition, the binding properties of the complex with CT-DNA were investigated by fluorescence and ultraviolet spectra. UV spectra indicate classical intercalation between the complex and CT-DNA. Moreover, the interactions between the ligand and the complex with CT-DNA were studied by EtBr fluorescence probe, which proved that these compounds bind to CT-DNA through an intercalation mode. The binding constants were 0.76 and 1.15 for Htfc and complex **1**, which means **1** has stronger interaction with CT-DNA than Htfc.

Keywords: 4-(trifluoro-methyl) nicotinic acid, crystal structure, DNA;
DOI: 10.14102/j.cnki.0254-5861.2011-3257

1 INTRODUCTION

Compounds composed of central metal ions and various multi-functional organic ligands have received increasing attention owing to their unique structural features and potential application in promising bioactive agents[1-3]. Complexes have been widely used in DNA structural probes[4, 5], molecular optical opening of DNA[6], footprint reagents of DNA[7] and fracture reagents of DNA[8, 9]. In addition, it has been widely accepted that DNA is the primary biological targets of many drugs in vivo[10]. Studies of the interaction between Cu(II) complexes and DNA have attracted great interest, because complexes with different crystal structures have different binding effects on DNA[11]. So far, a large number of Cu(II) compounds have been studied on their structures as well as physical and chemical properties[12, 13]. However, its relationships between structures and DNA interactions are still not particularly clear.

As one of the heterocycles, pyridine derivatives exhibit significant pharmacological activities like anticancer[14] and antibacteria[15] which are good ligand candidates. What's more, complexes constructed by fluorinated pyridine carboxylic acid ligands have already attracted much interest due to their extensive biological activity[16, 17]. They show a number of different coordination modes due to dual functionality of donor N atom which is a stabilizer of transition metal ions at lower oxidation state and O atom that is a stabilizer for transition metal in their higher oxidation states[18]. The introduction of fluorine could significantly enhance the chemical stability and bioactivity of the compounds[19-21]. So, 4-(trifluoro-methyl) nicotinic acid (Htfc) was chosen by us as a ligand, which can be regarded as an excellent building block for the construction of new coordination compounds[22].

Received 17 May 2021; accepted 26 July 2021 (**CCDC 2080477**)

① Supported by the National Natural Science Foundation of China (No. 21763022)

② Corresponding author. E-mail: mxiaoxia1222@163.com

In this work, a new complex $[Cu_{1.5}(tfc)_3(H_2O)_4]\cdot 3H_2O$ has been synthesized and characterized by X-ray single-crystal diffraction, elemental analysis and infrared spectra. The intercalation of the complex with CT-DNA was also studied by fluorescence and ultraviolet spectra methods which showed the reference value to the design of new drugs as well.

2 EXPERIMENTAL

2. 1 Materials and general methods

All chemicals were commercially available and used as purchased. Calf Thymus DNA (CT-DNA) and ethidium bromide (EB) were purchased from Sigma-Aldrich Co. Tris-HCl buffer solution (C = 0.1 mol·L^{-1}, pH = 7.4) was used for fluorescence spectrum. The concentration of CT-DNA was 200 g·mL^{-1} and stored at 4 ℃. The interactions between compounds and CT-DNA are measured using literature method[23]. Elemental analyses (C, H and N) were performed on a Vario EL III analyzer. Infrared spectra were obtained from KBr pellets on a BEQ VZNDX 550 FTIR instrument within the 400~4000 cm^{-1} region. Thermogravimetric analysis was carried out on a TA Instrument NETZSCH STA 449 C simultaneous TGA at a heating rate of 10 ℃·min^{-1} under hydrostatic air. Fluorescent data were obtained from a Hitachi F-7000 instrument. UV-vis spectral measurements for the synthesized complexes were made using a TU-1800 beam recording spectrophotometer.

2. 2 X-ray crystallography

Bruker Siemens Smart Apex II CCD diffractometer with graphite-monochromated Mo$K\alpha$ radiation (λ = 0.71073 Å) at 293(2) K. Cell parameters were retrieved using SMART software and refined using SAINTPLUS for all observed reflections. Data reduction and correction for ***Lp*** and decay were performed with the SAINTPLUS[24] software. Absorption corrections were applied using SADABS. All structures were solved by direct methods using SHELXS-97[25] and refined with full-matrix least-squares refinement based on F^2 using SHELXL-97[26]. For compound **1**, a total of 6471 reflections were collected in the range of $2.90 \leqslant \theta \leqslant 27.52°$, of which 4570 were independent (R_{int} = 0.0669). The final R = 0.0488 and wR = 0.1103 with $I > 2\sigma(I)$. The selected bond distances and bond angles are listed in Table 1.

Table 1. Selected Bond Lengths (Å) and Bond Angles (°) for Complex 1

Bond	Dist.	Bond	Dist.
Cu(1)–O(1)	2.003(2)	Cu(1)–O(7)	2.346(3)
Cu(1)–O(3)	2.001(2)	Cu(1)–O(8)	2.429(3)
Cu(1)–N(1)#1	2.002(3)	Cu(1)–N(2)#2	2.015(3)
Angle	(°)	Angle	(°)
O(1)–Cu(1)–O(7)	92.28(9)	O(3)–Cu(1)–N(2)#2	88.58(10)
O(1)–Cu(1)–O(8)	85.36(9)	N(1)#1–Cu(1)–N(2)#2	176.16(10)
O(3)–Cu(1)–N(1)#1	89.69(10)	N(1)#1–Cu(1)–O(1)	89.04(10)
O(3)–Cu(1)–O(1)	178.48(10)	N(1)#1– Cu(1)–O(8)	88.71(11)

Symmetry codes: #1: *x*, –*y*+3/2, *z* –1/2; #2: *x*, –*y*+1/2, *z*–1/2

2. 3 Synthesis of $[Cu_{1.5}(tfc)_3(H_2O)_4]\cdot 3H_2O$

A water solution (5 mL) of $Cu(NO_3)_2\cdot 2H_2O$ (24.16 mg, 0.1 mmol) was added to a solution of Htfc (9.50 mg, 0.05 mmol) in CH_3OH (10 mL) and water (5 mL). The pH of the mixture was adjusted to 9 by adding sodium hydroxide (0.5 mol·L^{-1}) with stirring. After *ca*. 30 min of vigorous mixing, the resulting solution was filtered and left to stand under ambient conditions. Upon slow evaporation of the solvents, blue transparent block crystals of complex were obtained after *ca*. 8 days in a yield of 68% (based on Htfc). Anal. calcd. for $C_{21}H_{17}Cu_{1.5}F_9N_3O_{10}$: C, 19.22; H, 1.11; N, 2.94%. Found: C, 19.20; H, 1.13; N, 2.96%. IR (KBr, cm^{-1}): 3431(w), 1633(s), 1375(s), 1281(m), 1193(w), 948(w), 848(w), 687(w), 470(w).

3 RESULTS AND DISCUSSION

3. 1 Structural description

Single-crystal X-ray diffraction analysis reveals that complex $[Cu_{1.5}(tfc)_3(H_2O)_4]\cdot 3H_2O$ crystallizes in the orthrohombic system, space group ***Pccn***. As shown in Fig. 1, Cu(II) ion is six-coordinated with two carboxylate oxygen atoms (O(1), O(3)) and two nitrogen atoms (N(1), N(2)) from the tfc$^-$ ligands as well as two oxygen atoms of coordination water molecules (O(7), O(8)), which resemble a slightly distorted

octahedral geometry. Two carboxylate oxygen atoms and two oxygen atoms from the coordination water molecule are in the equatorial plane (O(1), O(3), O(7) and O(8)). N(1) and N(2) from pyridine ring occupy the axial positions. As shown in Table 1, the Cu–O bond lengths range from 2.001(11) to 2.430(11) Å, while the distance of Cu–N(1) is 2.002(3) Å, which all fall in normal ranges[27]. The O–Cu–O bond angles vary from 89.95(10)° to 180.00(14)° and the N(1)–Cu(1)–N(2) bond angle is 176.16(11)°.

In this structure, the carboxylic groups and nitrogen atom in adjacent tfc^- ligands are linked to the Cu(II) ion, forming a 1D zigzag chain. Then, such 1D chains are connected into a 2D plain from tfc^- ligands with alternant 24-membered rings (Fig. 2).

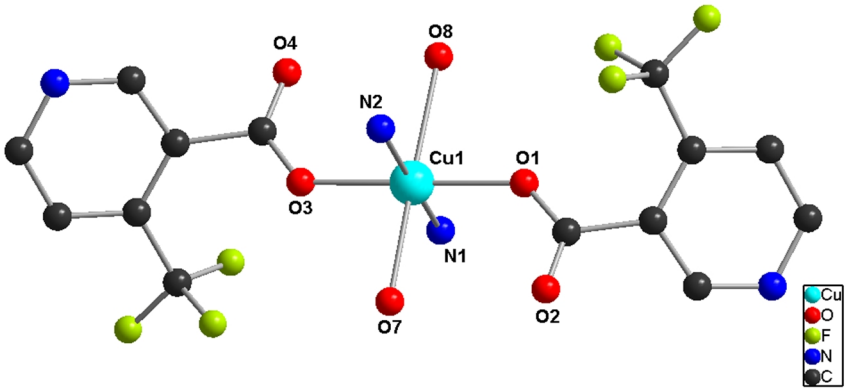

Fig. 1. Coordination environment of complex 1 (hydrogen atoms are omitted for clarity)

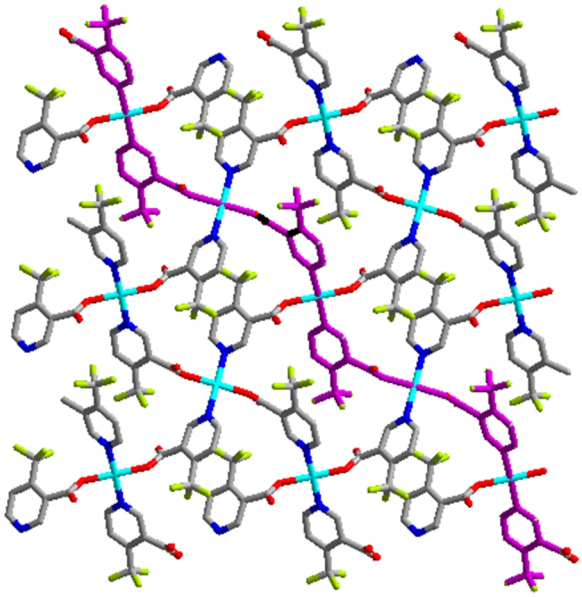

Fig. 2. 2D structure diagram in complex 1

3. 2 IR spectra

IR measurement has been performed between 400～4000 cm^{-1}. The IR spectrum of **1** shows a broad absorption band at 3431 cm^{-1}, corresponding to the O–H stretching of coordinated water molecules in the complex[28]. The C–N absorption peaks of pyridine can be observed at 1320 cm^{-1}. The $\nu_{asym}(COO^-)$ and $\nu_{sym}(COO^-)$ absorption can be observed as strong bands at 1633 and 1375 cm^{-1}, respectively. The $\Delta(\nu_{asym}(COO^-) - \nu_{sym}(COO^-))$ for **1** is 258 cm^{-1}, indicating that the coordination of carboxylate groups is closer to monodentate rather than to bidentate mode[29]. This result is in agreement with the crystal structure. These indicate that the carboxylic acid groups were converted into carboxylate anions due to the formation of the stable complex[30].

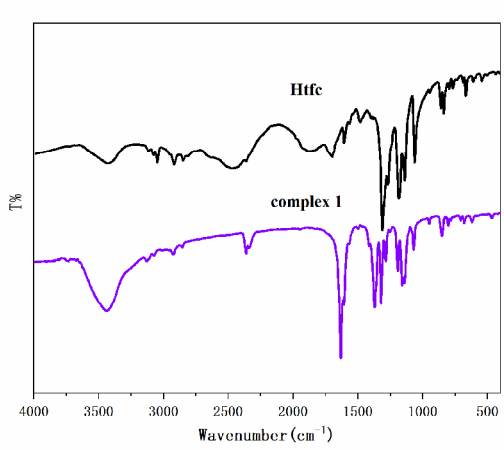

Fig. 3. IR spectra of Htfc and complex 1

3. 3 Thermogravimetric analysis

Thermogravimetric experiments were conducted to study the thermal stability of **1**, which is an important parameter for metal-organic framework materials. As shown in Fig. 4, the first weight loss of 7.6% in the range of 132.7～201.6 ℃ corresponds to the complete loss of four coordinated water molecules and three unbound water (calcd.: 8.2%). The main framework remains intact until heated to 338.5 ℃, and then releases all the ligands completely from 338.5 to 501.7 ℃, giving CuO as the final decomposition product with the residue percent of 14.3% (calcd.: 14.5%). The residual sample was characterized by X-ray powder diffraction (XRPD) at room temperature. As shown in Fig. 5, all diffraction peaks are in good agreement with the standard diffraction data for CuO (JCPDS card file No. 45-0937).

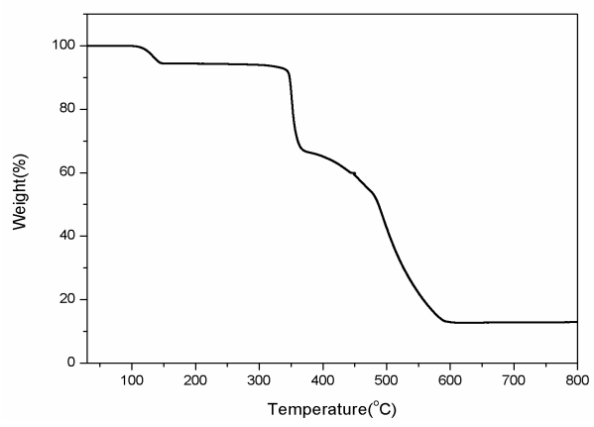

Fig. 4. TG curve of complex 1

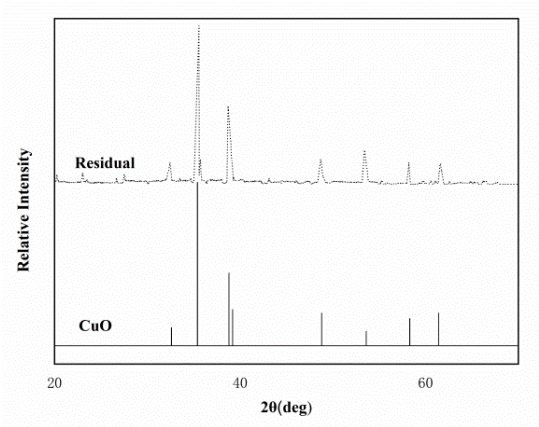

Fig. 5. XPRD patterns of the residual and CuO

3. 4 UV spectra

The UV-vis spectra are used to study the interactions of compounds with CT-DNA. As exhibited in Fig. 6, the absorption spectra were recorded at room temperature at 200~300 nm by keeping the concentration of complex (1×10^{-5}) while varying the CT-DNA concentration from 0, 2, 4, 6, 8 and 10 mol·L^{-1}. The absorbance of the complexes decreases obviously at 225 nm due to the π-π* transition of the pyridine ring[31]. With increasing the concentration of CT-DNA, a red-shift and hypochromic effect could be observed in the absorption of complexes, which may be attributed to accumulation of π electrons with the base pairs in the DNA structure, resulting in the subtractive effect and red shift of the absorption spectra[32]. Therefore, these changes indicate the classical intercalation mode between the complex and CT-DNA[33].

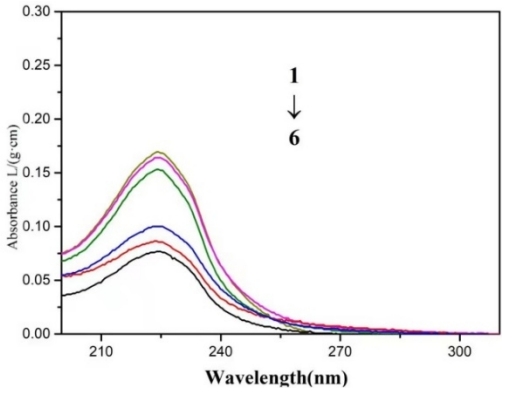

Fig. 6. Complex 1 of CT-DNA under UV spectra at different concentrations (compounds = 1 × 10^{-5} mol·L^{-1}; 10^{-5} C_{DNA}/(mol·L^{-1}) 1~6: 0, 2, 4, 6, 8, 10)

3. 5 EB-DNA binding study by fluorescence spectrum

Fluorescence spectroscopy has been used to investigate the interaction between the complex and DNA using ethidium bromide (EB) as a probe. EB is often used as a probe for spectroscopy studies of interactions between DNA and potentially embedded species[34]. Competitive binding of the complex to DNA and EB will result in the displacement of bound EB and a decrease in the fluorescence intensity. This property can be used to monitor the binding mode by the ability of a compound to prevent the intercalation of EB from DNA. For the fluorescence quenching experiments of the ligand and complex **1**, the EB solution was added to the prepared buffer solution of CT-DNA for 1 h and then added to the solution of the ligand and complex **1** from 0 to 10.3 μ mol·L^{-1}. An excitation wavelength of 520 nm was used and the emission spectra were recorded at 520~700 nm range. The peaks of ligand and complex were at 615 and 617 nm, respectively. Fig. 7 shows the effects of the ligand and complex **1** by steady state fluorescence emission experiments. The fluorescence intensity of EB-DNA system is weakening along with increasing the concentration of the ligand and complex **1**. It suggests that the compounds displaced EB from the CT-DNA-EB systems, and inserted into CT-DNA. In addition, the red shift of EB-DNA fluorescence peak occurred. It is caused by EB from the hydrophobic environment into hydrophilic, which further indicates that the tested compounds have intercalation with DNA[35].

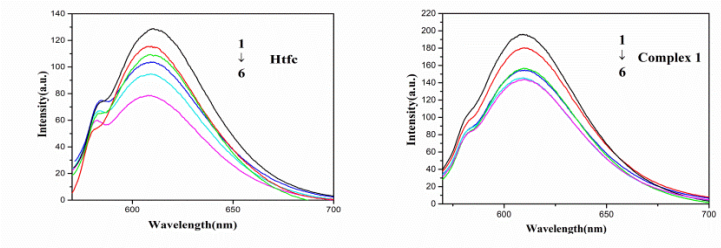

Fig. 7. Effects of Htfc and 1 on the fluorescence spectra of EB-DNA system (EB = 2 × 10^{-6} mol·L^{-1}; $10^{-5}C_{DNA}$ = 1.33 × 10^{-5} mol·L^{-1}; $10^{-6}C_{Htfc}$/(mol·L^{-1}) 1~6: 0, 1.0, 2.7, 5.0, 7.0, 10.3)

The classical *Stern-Volmer* equation is used to quantitatively determine the magnitude of the binding strength of the complex with CT-DNA[36]:

$I_0/I = 1 + K_{sq} R$

Where K_{sq} is a linear Stern-Volmer quenching constant and r is the concentration ratio of the quencher to CT-DNA , and I_0 and I represent the fluorescence intensities in the absence and presence of the quencher, respectively. The binding constants (K_{sq}) reveal the strength of the interaction between CT-DNA and the compounds. In the quenching plots of I_0/I versus r, the K_{sq} values were given by slopes. Usually, a bigger binding constant means a greater binding affinity to the CT–DNA. Thus, the K_{sq} value of complex **1** was 1.15, which is much higher than the ligand (0.76). The results show that the interactions of complex **1** with CT-DNA are stronger than the ligand probably due to the structure rigidity and metal-ligand synergism effect of **1**[37]. In addition, the introduction of trifluoromethyl group enhances the water solubility and lipophilicity of complex **1**, thereby heightening its biological activity[38].

4 CONCLUSION

In conclusion, a new complex $[Cu_{1.5}(tfc)_3(H_2O)_4]\cdot 3H_2O$ has been successfully synthesized from a novel picolinic acid ligand of Htfc = (4-(trifluoromethyl) nicotinic acid). The structure was characterized by X-ray single-crystal diffraction, elemental analysis, IR spectra and thermogravimetric analysis. The neighboring 1D chains are connected into a 2D structure through bridge connection from the tfc^- ligands. In addition, the interactions of the ligand and **1** with CT-DNA have been investigated through fluorescence and ultraviolet spectra, which declared the intercalation mode of CT-DNA by the ligand and **1**. The results were expected to give some significant insight into the interactions of transition metal complexes and CT-DNA, which show great reference value for a model of application for drug design.

REFERENCES

(1) Jessica, Z. C.; Ahmet, Y.; Min, C.; Zhang, Y. Y.; Zhang, B. C.; Wasa, M. Direct conversion of n-alkylamines to n-propargylamines through C−H activation promoted by Lewis acid/organocopper catalysis: application to late-stage functionalization of bioactive molecules. *J. Am. Chem.Soc.* **2020**, 142, 16493−16505.

(2) Deng, Z. Y.; Pei, Y. Q.; Wang, S. S.; Zhou, B.; Hou, X. Y.; Li, J.; Li, B.; Liang, H. S. Designable carboxymethylpachymaran/metal ion architecture on sunflower sporopollenin exine capsules as delivery vehicles for bioactive macromolecules. *J. Agric. Food. Chem.* **2020**, 68, 13990−14000.

(3) Woods, J. J.; Cao, J.; Lippert, A. R. Characterization and biological activity of a hydrogen sulfide-releasing red light-activated ruthenium(II) complex. *J. Am. Chem. Soc*. **2018**, 140, 12383−12387.

(4) Zakhar, V. R.; Vladimir, A. P.; Marina, A. K.; Andrey, A. B.; Alexei, I. K. Structure and formation of luminescent centers in light-up ag cluster-based DNA probes. *J. Phys. Chem. C* **2021**, 125, 3542−3552.

(5) Mardanya, S.; Srikanta, K.; Debiprasad, M.; Sujoy, B. Homo- and heterobimetallic ruthenium(II) and osmium(II) complexes based on a pyrene-biimidazolate spacer as efficient DNA-binding probes in the near-infrared domain. *Inorg. Chem.* **2016**, 55, 3475−3489.

(6) Izabela, K.; Johann, B.; Sebastian, M.; Philip, T. Strong plasmonic enhancement of a single peridinin-chlorophyll a-protein complex on DNA origami-based optical antennas. *ACS. Nano.* **2018**, 12, 1650−1655.

(7) Lori, M. O.; Thomas, D.; Tullius, M. High-resolution in vivo footprinting of a protein-DNA complex using γ-radiation. *J. Am. Chem. Soc.* **2000**, 122, 5901−5902.

(8) Spence, P.; Fielden, J.; Waller, Z. A. E. Beyond solvent exclusion: i-motif detecting capability and an alternative DNA light-switching mechanism in a ruthenium(II) polypyridyl complex. *J. Am. Chem. Soc*. **2020**, 142, 13856−13866.

(9) Simon, J.; Stammler, A.; Oldengott, J.; Bögge, H.; Glaser, T. Proof of phosphate diester binding ability of cytotoxic DNA-binding complexes. *Inorg. Chem.* **2020**, 59, 14615−14619.

(10) Li, X.; Luo, X. J.; Yang, Y.; Ma, L.; Wang, S. L.; Luo, Z. H. Synthesis, structure, and DNA binding of a platinum(II) complex based on the 3,4,5-trimethoxy-phenyl-1H-imidazo[4,5-f][1,10]phenanthroline. *Chin. J. Struct. Chem*. **2018**, 37, 811−818.

(11) Liu, Y. Z.; Gao, H. Y.; Yi, X. G.; Li, D. P.; Li, Y. X. Crystal structures and DNA binding properties of 2-naphthoxyacetic acid Cu(II) complexes. *Chin. J. Struct. Chem.* **2019**, 8, 1362−1369.

(12) Jana, S.; Ray, A.; Chandra, A.; Fallah, M. S. E.; Das, S.; Sinha, C. Studies on magnetic and dielectric properties of antiferromagnetically coupled dinuclear Cu(II) in a one-dimensional Cu(II) coordination polymer. *ACS. Omega.* **2020**, 5, 274−280.

(13) Schneider, J. D.; Smith, B. A.; Williams, A. G.; Powell, R. D.; Perez, F.; Rowe, T. G.; Lei, Y. Synthesis and characterization of Cu(II) and mixed-valence Cu(I) Cu(II) clusters supported by pyridylamide ligands. *Inorg. Chem.* **2020**, 59, 5433−5446.

(14) Gould, N. S.; Xu, B. J. Temperature-programmed desorption of pyridine on zeolites in the presence of liquid solvents. *ACS. Catal*. **2018**, 8, 8699−8708.

(15) Mugnaini, C.; Kostrzewa, M.; Kostrzewa, M.; Mahmoud, M. A.; Brizzi, A.; Lamponi, S.; Giorgi, G.; Ferlenghi, F.; Vacondio, F.; Maccioni, P.; Colombo, G.; Mor, M.; Starowicz, K.; Marzo, D. V.; Ligresti, A.; Corelli, F. Design, synthesis, and physicochemical and pharmacological profiling of 7-hydroxy-5-oxopyrazolo[4,3-b]pyridine-6-carboxamide derivatives with antiosteoarthritic activity in vivo. *J. Med. Chem.* **2020**, 63, 7369−7391.

(16) Li, B.; Wang, J. K.; Song, H.; Wu, H. P.; Chen, X. Y.; Ma, X. X. Synthesis, crystal structure, and BSA interaction with a new Co(II) complex based on 5-(trifluoromethyl)pyridine-2-carboxylic acid. *J. Coord. Chem.* **2019**, 166, 38−36.

(17) Vadori, M.; Pacor, S.; Vita, F.; Zorzet, S.; Cocchietto, M.; Sava, G. Features and full reversibility of the renal toxicity of the ruthenium-based drug NAMI-A in mice. *J. Inorg. Biochem.* **2013**, 118, 21−27.

(18) Wang, J. K.; Li, B.; Wu, H. P.; Tian, X. Y.; Ma, X. X. Synthesis, crystal structure and DNA-binding property of a Mn(II) complex based on 5-(trifluoromethyl)pyridine-2-carboxylic acid. *Chin. J. Struct. Chem.* **2019**, 8, 1349−1355.

(19) Swanson, D. M.; Dubin, A. E.; Shah, C. Identification and biological evaluation of 4-(3-trifluorom ethylpyridin-2-yl)piperazine-1-carboxylic acid (5-trifluoromethylpyridin-2-yl)amide, a high affinity TRPV1 (VR1) vanilloid receptor antagonist. *J. Med. Chem.* **2005**, 48, 1857–1872.

(20) Asahina, Y.; Araya, I. I.; Wase, K. Synthesis and antibacterial activity of the 4-quinolone-3-carboxylic acid derivatives having a trifluoromethyl group as a novel N-1 substituent. *J. Med. Chem.* **2005**, 48, 3443–3446.

(21) Akher, B. F.; Farrokhzadeh, A.; Ravenscroft, N.; Kuttel, M. M. Mechanistic study of potent fluorinated EGFR kinase Inhibitors with a quinazoline scaffold against L858R/T790M/C797S resistance mutation: unveiling the fluorine substituent cooperativity effect on the inhibitory activity. *J. Phys. Chem.* **2020**, 124, 5813−5824.

(22) Shang, Y.; Feng, X.; Li, J.; Wang, Y.; Wang, L.; Li, Z. Tow novel hydroxide anions bridged lanthanide coordination polymers based on fluorinated carboxylate ligand: structures, luminescence and magnetic property. *Inorg. Chem. Commun*. **2019**, 105, 47−54.

(23) Morya, V.; Walia, S.; Mandal, B. B.; Ghoroi, C.; Bhatia, D. Functional DNA based hydrogels: development, properties and biological applications. *ACS. Biomater. Sci. Eng.* **2020**, 6, 6021−6035.

(24) Sheldrick, G. M. *SADABS. Program for Empirical Absorption Correction of Area Detector.* University of Göttingen, Germany **1996**.

(25) Sheldrick, G. M. *SHELXL-97, Program for the Crystal Structure Refinement*. University of Göttingen, Germany **1997**.

(26) Sheldrick. G. M. *SHELXL-2014, Program for Crystal Structural Refinement.* University of Göttingen, Germany 2**014**.

(27) Iqbal, M.; Ali, S.; Tahir, M. N. Octahedral copper(II) carboxylate complex: synthesis, structural description, DNA-binding and anti-bacterial studies. *J. Coord. Chem.* **2018**, 71, 991−1002.

(28) Ren, J. L.; Jin, X. D.; Qiu, J. R.; Liang, H. J.; Li, B. A new Co(II) coordination compound constructed by tripyridyltriazole and pyromellitic acid: synthesis, crystal structure and antifungal activity. *Chin. J. Struct. Chem.* **2017**, 36, 33−39.

(29) Lim, E. K.; Teoh, S. G.; Goh, S. M.; Ch'ng, C. D.; Ng, C. H.; Fun, H. K.; Rosli, M. M.; Najimudin, N.; Beh, H. K.; Seow, L. J.; Ismail, N.; Ismail, Z.; Asmawi, M. Z.; Cheah, Y. H. Characterization, nucleolytic, cytotoxic and antibacterial property of tetrakis(μ-4-chloro-2-nitrobenzoato-k^{2}O,O′)) bis[aquacopper(II)], tetrakis(μ-2-chloro-6-fluorobenzoato-k^{2}O,O′)bis[aquacopper(II)] and tetrakis(μ-2-chlorobenzoato-k^{2}O,O′)bis[aquacopper(II)]. *Polyhedron* **2009**, 25, 1320−1330.

(30) Ren, Y. W.; Hu, H. N.; Zhang, J.; Zhuang, X. J.; Li, D. P.; Li, Y. X. Characterization and DNA interaction of lanthanide complexes based on thiourea ligand. *Chin. J. Struct. Chem.* **2021**, 40, 47−54.

(31) Marjolein, E. Z.; Velthoen, S. N.; Bert, M. W. Probing acid sites in solid catalysts with pyridine UV-Vis spectroscopy. *Phys. Chem. Chem. Phys*. **2018**, 20, 21647.

(32) Totta, X.; Hatzidimitriou, A. G.; Papadopoulos, A. N. Nickel(II)-naproxen mixed-ligand complexes: synthesis, structure, antioxidant activity and interaction with albumins and calf-thymus DNA. *New. J. Chem.* **2017**, 41, 4478−4492.

(33) Jain, S.; Khan, T. A.; Patil, Y. P. Bio-affinity of copper(II) complexes with nitrogen and oxygen donor ligands: synthesis, structural studies and in vitro DNA and HSA interaction of copper(II) complexes. *J. Photochem. Photobiol. B* **2017**, 174, 35−43.

(34) Liu, Y. Z.; Gao, H. Y.; Yi, X. G.; Li, D. P.; Li, Y. X. Crystal structures and DNA binding properties of 2-naphthoxyacetic acid Cu(II) complexes. *Chin. J. Struct. Chem.* **2019**, 38, 1362−1369.

(35) Iqbal, M.; Ali, S.; Rehman, Z.; Muhammad, N.; Sohail, M.; Pandarinathan, V. Synthesis, crystal structure description, electrochemical, and DNA binding studies of "paddlewheel" copper(II) carboxylate. *J. Coord. Chem.* **2014**, 67, 1731−1745.

(36) Mcmillan, D. R.; Mcnett, K. M. Photoprocesses of copper complexes that bind to DNA. *Chem. Rev.* **1998**, 3, 1201−1220.

(37) Liu, W. Q.; Zhou, S. L.; Fan, M. Z.; Pan, Z. Q.; Chen, Y. F. Synthesis and crystal structure of a dinuclear Cu(II) complex based on a carboxyl-substituted1H-1,2,3-triazole and its DNA cleavage activity. *Chin. J. Struct. Chem.* **2015**, 6, 917−924.

(38) Yang, M. Y.; Zhai, Z. W.; Sun, Z. H. A facile one-pot synthesis of novel 1,2,4-triazolo[4,3-a]pyridine derivatives containing the trifluoromethyl moiety using microwave irradiation. *J. Chem. Res.* **2015**, 39, 521−523.